

# A High-Precision Low-Cost Analog Acceleration and Vibration Amplifier using PVDF Piezoelectric Sensors

Thomas L. Hemminger<sup>1</sup>

<sup>1</sup> The Behrend College

*Received: 13 June 2021 Accepted: 5 July 2021 Published: 15 July 2021*

---

## Abstract

This paper describes a high-resolution analog acceleration and vibration amplifier for use with piezoelectric polyvinylidene fluoride (PVDF) sensors. The purpose of this system is to monitor automated parts placement on integrated circuit boards. One of the problems facing production and inspection equipment is the occurrence of resonant and ambient vibrations. Even small errors can cause systems with micrometer and nanometer precision to exceed design tolerances. This work describes a method to monitor mechanical vibrations through a portable and inexpensive signal-processing unit. The system provides user-selectable gain and filtering modules that are compact and reliable. PVDF is currently used in sensing applications, and its material properties have proven very useful for sensing mechanical stress, strain, pressure, and temperature

---

*Index terms*— PVDF, piezoelectric film, vibration sensing, Sallen-Key

## 1 Introduction

As the integration level of electronic systems increases and becomes more sophisticated, producing these devices grows more complicated and expensive. Not only does fabrication become increasingly difficult, but inspection and testing are also more demanding. One of the problems facing automated production and inspection equipment is resonant and ambient vibration. The design described here was motivated by the specific needs of an industrial sponsor. However, it can be useful for many applications requiring low-cost sensors for monitoring vibrations and accelerations. Polyvinylidene Fluoride (PVDF) is an extremely effective material for converting mechanical movements into electrical signals and has some of the strongest piezoelectric effects of all known polymers [1]. This property makes the material an effective candidate for use in the construction of vibration and acceleration sensors [2]- [7]. There are, however, some disadvantages when working with PVDF. Not only does it exhibit a high piezoelectric constant, but also a considerable pyroelectric constant, indicating that the material produces high voltage variations when exposed to changes in temperature. There can be as much as an 8-volt change in output voltage per degree Celsius [8]. This can be managed with a combination of shielding and a DC offset control. PVDF material is also highly capacitive and is sensitive to IR and RF interference, but careful design can reduce these effects. All of these potential problems were considered and addressed in the finished system.

Initially, several currently available designs were evaluated to investigate the properties of PVDF sensors and the signal processing characteristics of the associated amplifiers [9]. Improved amplification and conditioning circuitry was designed, constructed, and tested for use with several types of these sensors. Frequency response, dynamic range, and measurement axes are important, but cost is another important factor. The analog system described here is robust, low-cost, and portable. It can employ batteries, a single +5volt supply, or a plug-in wall adapter. Excessive vibrations are indicated through a simple LED arrangement, or the system can be connected to a data acquisition recorder for time and/or frequency analysis. The specifications for the overall system are illustrated in Table 1.

## 2 System Design

This design is composed of seven blocks, which are described in the following subsections. The high-pass and low-pass filters are of similar configuration. Therefore, only the high-pass filters will be described in detail. Component values are included for all of the filtering elements. A block diagram of the conditioner is shown in Fig. ???. One specification required of this design is that it operates from a single 5-volt DC power supply. Therefore, a Newport NMA0512S one-watt to DC-to-DC converter was employed to power all components. This model has an internal oscillation frequency of 100 kHz, which is well beyond the frequency ranges being monitored. The low-power design presented here lends itself to battery operation, which is advantageous over plug-in wall adapters because of AC line interference.

### 3 b) Input impedance control

High input impedance is necessary to successfully measure PVDF sensor signals at low frequencies. This is due to the capacitance characteristics of the film [10][11]. The capacitance of PVDF is a function of its geometry, indicating that the cutoff frequency is usually determined by the amplifier input impedance alone ( $f_c = 1/2\pi RC$ ). For example, if an amplifier has an input impedance of 10k $\Omega$  for a given PVDF capacitance of 3nF it yields a cutoff frequency of 5.3kHz which is unacceptable for this application. One goal is to amplify signals of very low frequency near the DC level. To achieve lower cutoff frequencies the input resistance of the amplifier must be increased. Consequently, a non-inverting JFET voltage follower with an input impedance of about 10 $^{12}$   $\Omega$  was chosen to enable measurements at very low frequencies. This produces a cutoff frequency of about  $5.3 \times 10^{-5}$  Hz. The drawback to a non-inverting buffer is that input bias currents of the op-amp cause the amplifier to saturate. This condition can be alleviated by providing another high impedance path to ground (see Fig. 2). The value of R must be high enough to provide a cutoff frequency below the lowest frequency of interest. For example, to achieve a cutoff frequency of 10 Hz with a sensor that has a capacitance of 3nF would require a 5.3M $\Omega$  resistor. For this example, R = 50 M $\Omega$  which results in a cutoff frequency of about 1 Hz which fits the required specifications. The impedance control resistor determines the input impedance of the buffer so this resistance should be chosen with knowledge of the physical characteristics of the sensors to be used with the system.

### 4 Fig. 1: High-level design of the signal conditioner

Because of the possibility of high voltage spikes from PVDF sensors, the design includes two zener diodes to regulate the input signal. Diodes should be chosen with breakdown voltages higher than the opamp supply voltage. For the prototype amplifier, zener diodes with a 20V breakdown voltage were selected. G-force amplitudes and corrupting frequencies have been a concern. Therefore it was decided to have a selectable frequency range via switches on the circuit board. A range of high-pass and low-pass filters in a cascade arrangement was decided upon, each having the ability to be independently activated. The low-pass cutoff frequencies were 100 Hz, 500 Hz, 1 kHz, and 10 kHz. The high-pass cutoffs were 3Hz, 100 Hz, 500 Hz, and 1 kHz. With this design the user may select 15 combinations of high-pass and low-pass filters. An "allpass" switch has been included in both filter banks as a bypass. The LF347 op-amp was chosen because it has several useful features, e.g., extremely high input impedance (10 $^{12}$   $\Omega$ ), low input bias current (50 pA), and wide bandwidth (4 MHz).

## 5 Input

Several active filter models were investigated, but after reviewing the tradeoffs, the Sallen-Key configuration was most suitable [12] [13] [14]. The highfrequency specification for this system is 10 kHz, which is well below the 1 MHz level at which this filter begins to degrade. Also, since the amplification is done in a separate circuit, all filter stages are unity gain, alleviating gain-bandwidth product issues. Filter selectivity is certainly an important factor but linear phase response is also significant, so only two filter families were explored i.e., Butterworth and Bessel. The Butterworth has a much stronger roll-off than the Bessel, but the phase response is not as flat. However, Bessel filters have such a gradual roll-off that the required order becomes prohibitive. Also, as shown in Fig. 3, the phase response of the Butterworth is nearly linear in the passband, translating into an acceptable group delay. Further examination of the delay shows us that it has little effect on the output of the filters. The delay is uniform through the majority of the pass-band-up approximately 4 kHz for 4th order. This was verified by comparing the total harmonic distortion of these two filters at frequencies near the cutoff. For 5 kHz, 9 kHz, and 10 kHz input signals the THD of both filter types is less than 0.006%. For these reasons the Butterworth was chosen. (1) (2) Each filter used in this project comprises two cascaded 2-pole filters, yielding a 4-pole configuration with all filters designed to have less than 0.5 dB attenuation in the pass-band.

Fig. 4 illustrates the layouts of the high-pass and low-pass 4-pole Sallen-Key filters. Values for all resistive and capacitive components are shown in table 2. Because the input to the high-pass filters is linked directly to the impedance control circuit, this is the optimum place to remove any DC offset, which may be present in the input. For this reason a low voltage DC offset adjustment was added to the non-inverting terminal of the summing amplifier (Fig. ??). This circuit allows any small op-amp bias voltages to be removed from the output of the summing amplifier before proceeding to the gain control, and possibly corrupting the output. The low-pass filter selection circuitry is nearly identical to that of the high-pass block. The only

101 1 1 1 1 ) ( R R C C R C K R C R C s s R R C C K s H + ? ? ? ? ? ? ? + + + = 2 2 1 2 1 2 2 1 2 1 2 1 2 1 2  
 102 1 1 1 ) 1 ( ) ( 1 ) ( s R R C C s C C R R K C R C C R K s H c c ? + ? ? + + + = ? ?  
 103 difference is that the DC offset control is not present because any significant offsets will have been removed  
 104 in the high-pass stage. The switches used to operate the selection circuitry are of the double pole single throw  
 105 slide type. The center tap of the switch is connected to the input of a classic summing amplifier, which is shown  
 106 in Fig. ???. The other two terminals are connected to the outputs of their respective filters and to ground. The  
 107 ground, or off position, assures that none of the inputs to the summing amplifier are left floating.

## 108 6 d) Amplifiers

109 The amplification circuit is composed of a simple inverting op-amp. Several other circuits were considered, but  
 110 the inverting op-amp was selected for its ease of implementation, small number of components, and input/output  
 111 impedance characteristics. For added versatility, the gain of the inverting op-amp is controlled by shorting a  
 112 series of resistors in the feedback loop of the amplifier. By connecting the resistors in series, a wide range of gains  
 113 can be selected. As illustrated in Fig. ?? this circuit employs 10 k?, 50 k?, 100 k?, 500 k?, and 1 M? resistances  
 114 allowing for gains ranging from 1X to 166X. The gain is controlled via switches that short various resistors. For  
 115 example, shorting the 500 k? and 1 M? resistors yields a gain of 1X+5X+10X for a total of 16X.

116 Fig. ???: Amplifier variable gain circuit. Note: The LF347 op-amp was used for testing purposes e) Output  
 117 A visual display was added to the amplifier to alert the user of the presence of excessive g-forces. This simple  
 118 readout eliminates the need to use an oscilloscope to view the output when portability is an issue. The method  
 119 chosen to accomplish this task was the illumination of three LEDs. Yellow, green and red LEDs illuminate when  
 120 the output of the amplifier reaches a peak value of one, seven, and ten volts respectively. Two sets of LEDs  
 121 were used to indicate positive and negative g-forces. The circuit is illustrated in Fig. 8. The input is isolated  
 122 by using an op-amp buffer to assure that the rectifier circuit does not interfere or load the output. It should  
 123 be noted that the output of the rectifier circuit is not exactly equal to the peak AC value of the input due to  
 124 the approximate 0.6V drop over the diode. This drop must be accounted for when designing the comparator  
 125 circuit that lights the LEDs. The visual display circuits compare the DC voltage from the rectifier circuits with  
 126 a predetermined threshold voltage. Operational amplifiers were employed here as well for design simplicity and  
 127 to reduce component count.

## 128 7 Results

129 Multiple mechanical frequencies must be utilized to test the accuracy of the filters and the sensitivity of the  
 130 amplifier. To achieve clean consistent vibration signals, an aluminum cantilever beam was used to create  
 131 vibrations and accelerations of varying amplitude and frequency (see Fig. ??). Testing of low frequencies was  
 132 accomplished using the cantilever beam, while high-frequency testing was completed using an electrodynamic  
 133 shaker.

## 134 8 Fig. 9: The cantilever beam setup for low frequency testing

135 To analyze the functionality of the amplifier in a time-efficient manner, the output of the sensors was read through  
 136 a data acquisition system for comparative purposes. This test arrangement was composed of the amplifier, a  
 137 Keithley data acquisition board, and a computer running National Instruments' Lab VIEW software.

138 As with most signal amplifiers, linearity is a significant factor in this design, therefore two tests were employed  
 139 to verify the efficacy of each stage. Initially, the amplifier was set to 1X gain with all filters bypassed. The input  
 140 voltage was incrementally increased from 0V to 10V while recording the outputs and calculating the respective  
 141 correlation coefficients. The test was repeated with one high-pass and one low-pass filter activated to validate  
 142 the filter circuits. The process was then repeated for numerous combinations being careful not to saturate each  
 143 stage. The worst-case deviation from linearity is illustrated in Fig. 10. With a 1X gain selected, the upper 3dB  
 144 point of the amplifier is 220 kHz. With the gain set at 166X, the 3dB point is shifted to 18 kHz, reducing the  
 145 operating bandwidth as expected, but still remaining within the design limits. The 3dB point for each filter was  
 146 within 5% of the calculated value, and the roll-off rates exceeded 65 dB/decade. In order to scale the output  
 147 correctly the gain values must be accurately known, otherwise significant errors will result when calculating the  
 148 acceleration or vibration magnitudes. All five gain switches were toggled to determine the influence of each. The  
 149 results are summarized in table 3. Small deviations from the predicted values can be attributed to component  
 150 variations but are still within design limits. All goals of table 1 were accomplished or exceeded.

## 151 9 Conclusion

152 An alternative technique for analyzing signals from PVDF sensors has been introduced and this signal conditioning  
 153 system has proven to be useful, inexpensive, and relatively easy to fabricate. It also provides reliable and  
 154 repeatable results for several PVDF sensor models. With the output connected to an analog-to-digital converter  
 155 card the signal processor described here exceeded the capabilities of similar products tested. This conditioner  
 156 adds several useful features to comparable products such as a selectable gain, high-pass and low-pass filters, and  
 157 a simple output indicator. This amplifier is an excellent alternative to comparable designs but at a significantly  
 158 reduced cost. Its versatility makes it suitable for use with most PVDF sensors. This work was initiated from

## 9 CONCLUSION

159 an industrial need for a simple and reliable acceleration and vibration signal conditioning system for automated  
160 integrated circuit placement, still there can be many other uses, e.g., impact sensors, flow meters, contact  
161 microphones, etc. Several sensors can be connected to similar conditioners, and by simultaneously monitoring  
the outputs of two or more devices, one can gain a better understanding of where vibrations are originating.

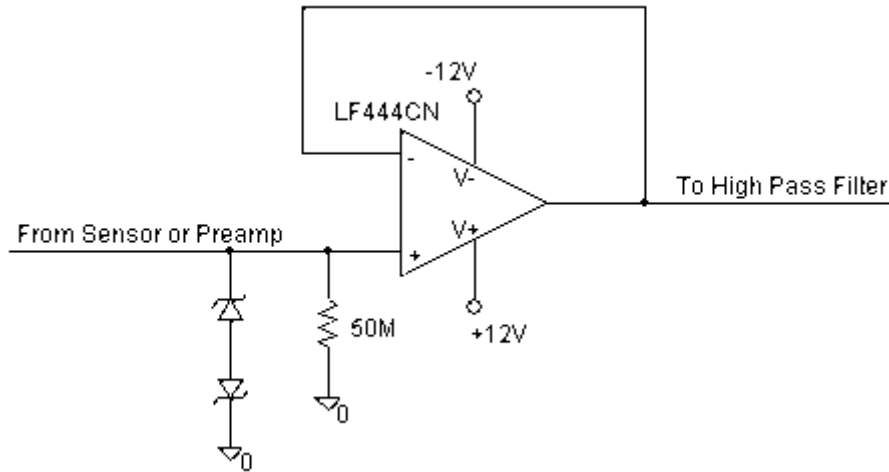


Figure 1: Fig. 2 :

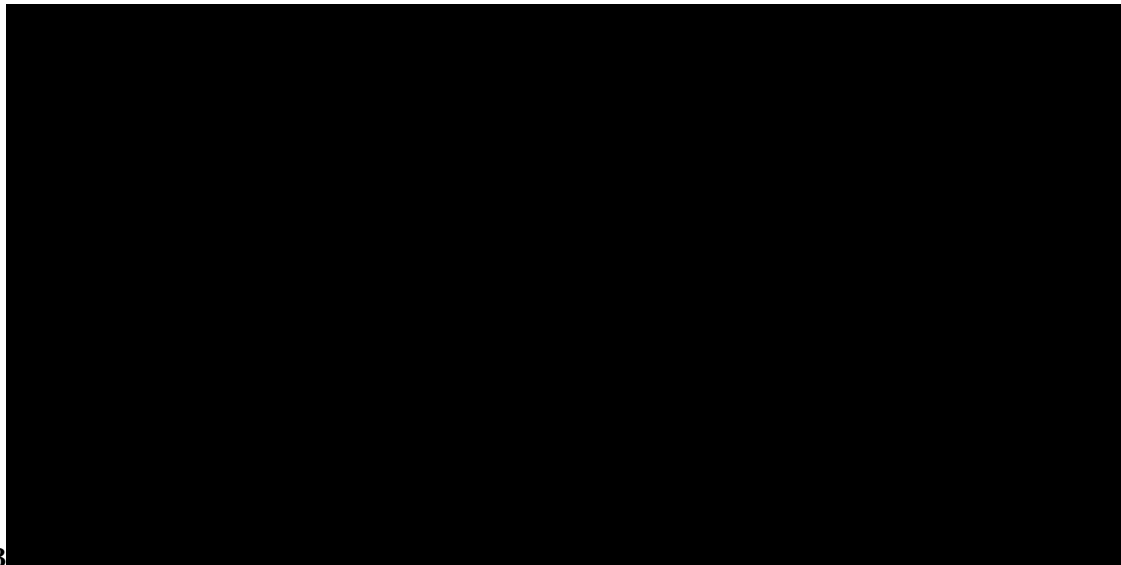


Figure 2: Fig. 3 :

162 1 2 3 4  
163

<sup>1</sup>( ) F © 2021 Global JournalsA High-Precision Low-Cost Analog Acceleration and Vibration Amplifier using PVDF Piezoelectric Sensors

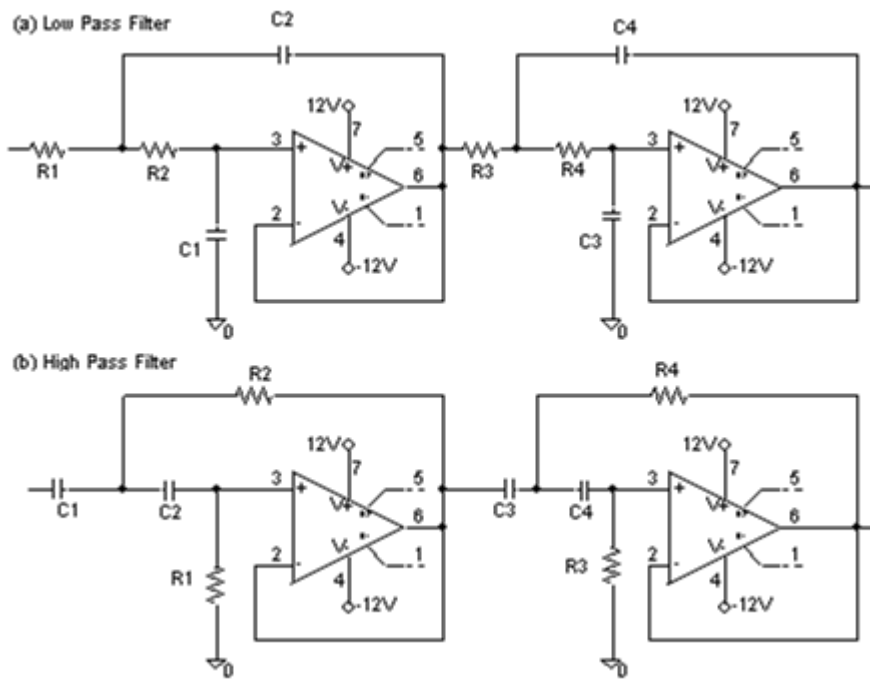
<sup>2</sup>© 2021 Global Journals

<sup>3</sup>( ) F © 2021 Global Journals

<sup>4</sup>A High-Precision Low-Cost Analog Acceleration and Vibration Amplifier using PVDF Piezoelectric Sensors

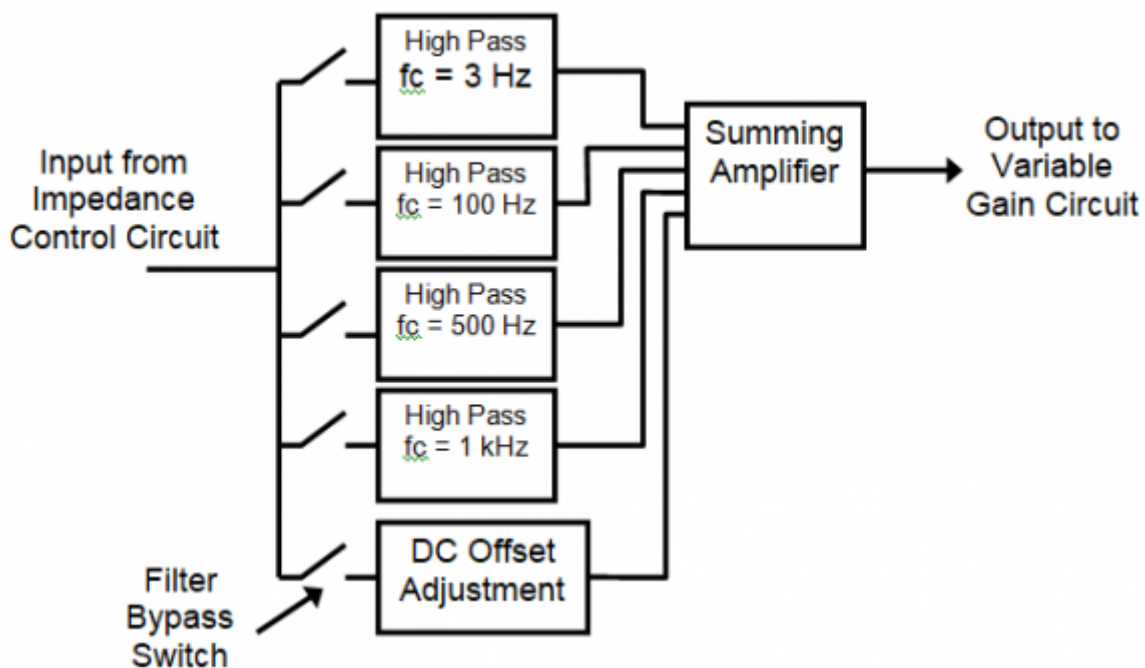


Figure 3: Fig. 4 :



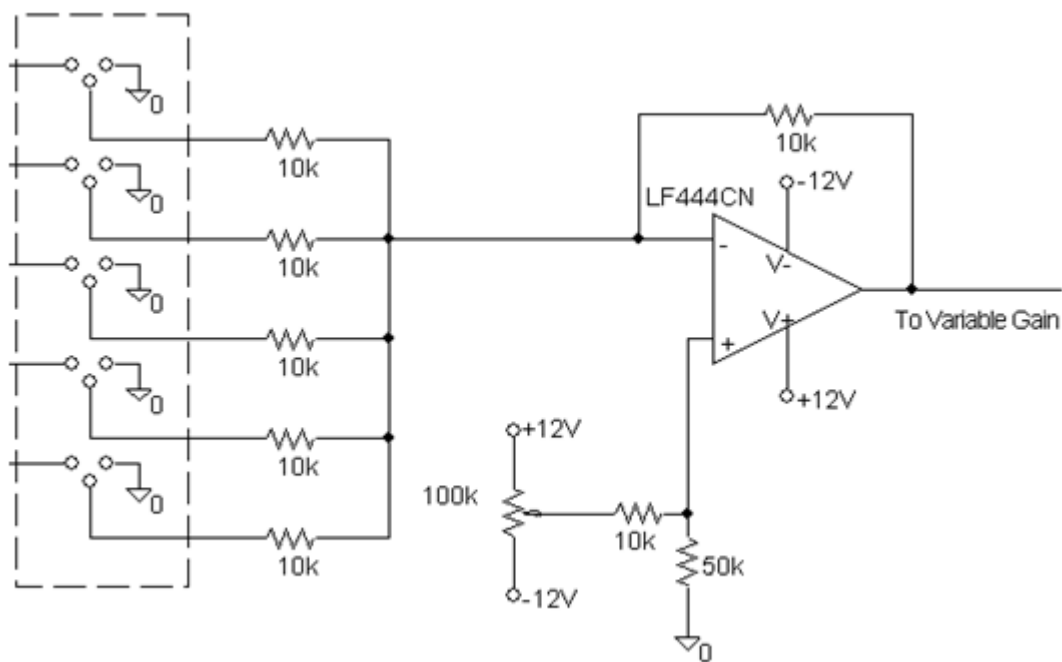
56

Figure 4: Fig. 5 :Fig. 6 :



8

Figure 5: Fig. 8 :



10

Figure 6: Fig. 10 :

1

Parameter	Specification
Frequency Range	0 Hz to 10 kHz, at selectable ranges
Filter roll-off	60 dB/decade
THD	<0.02%
Linearity	<0.2% deviation
Resolution	1 . 0 $\mu$ g / Hz in conjunction with sensor
Gain	Selectable up to 150
Thermal Stability	Minimal effect
Dynamic Range	$\pm$ 50 g
Transverse Sensitivity	< 1%
Output	+/-10V

Figure 7: Table 1 :

2

Freq.	R1	R2	R3	R4	C1	C2	C3	C4
Low- 100 Hz	2.32 k?	21.2 k?	18.2 k?	18.9 k?	1.0 nF	3.3 nF	470 pF	10 nF
Pass 500 Hz	1.66 k?	16.3 k?	2.33 k?	19.0 k?	6.8 nF	22 nF	3.3 nF	22 nF
1 kHz	2.18 k?	18.4 k?	1.59 k?	17.2 k?	22 nF	68 nF	10 nF	220 nF
10 kHz	8.93 k?	37.5 k?	3.55 k?	18.9 k?	20 nF	220 nF	100 nF	220 nF
High-3 Hz	17.6 k?	15.0 k?	42.4 k?	6.21 k?	3.3 $\mu$ F	3.3 $\mu$ F	3.3 $\mu$ F	3.3 $\mu$ F
Pass 100 Hz	15.5 k?	11.3 k?	26.6 k?	3.89 k?	220 nF	100 nF	220 nF	220 nF
500 Hz	4.85 k?	4.14 k?	14.5 k?	2.04 k?	100 nF	100 nF	100 nF	68 nF
1 kHz	2.43 k?	2.07 k?	16.2 k?	1.40 k?	100 nF	100 nF	100 nF	22 nF

Figure 8: Table 2 :

3

Vin	Vout	Gain	Actual Gain	%error
1.525	1.55	1	1.016	3.25%
0.31	1.575	5	5.081	1.59%
0.135	1.375	10	10.18	1.82%
0.105	5.2	50	49.52	-0.96%
0.0525	5.1	100	97.14	-2.94%
0.052	8.625	166	165.8	-0.08%

Figure 9: Table 3 :

4

Parameter	Measured Results	
Frequency Range	0 Hz to 10 kHz, at selectable ranges	
Filter roll-off	>65 dB/decade	
THD	<0.012%	
Linearity	0.11% deviation	
Resolution	04 0 $\mu$ . g	Hz in conjunction with sensor
	/	
Gain	Selectable up to 166	
Thermal Stability	Minimal effect	
Dynamic Range	>	50 g
Transverse Sensitivity	< 1%	
Output	+/-10V	
IV.		

Figure 10: Table 4 :



- 
- 164 [Kimoto and Sugitani] ‘A multifunctional Tactile Sensor Based on PVDF Films for Identification of Materials’  
165 Kimoto , Fujisaki Sugitani . *IEEE Sensors Journal* 10. (Issue 9)
- 166 [Hill and Horwitz] *Art of Electronics 13*, Winfield Hill , Paul Horwitz . Dorf, Richard C..
- 167 [Ting et al. ()] ‘Circuitry Design for Direct Wind Energy Harvest System’. Y Ting , C Chang , H Gunawan .  
168 *IEEE International Symposium on Industrial Electronics*, 2010.
- 169 [Hutchinson] *Design of self Calibrating Piezoelectric Polymer Based Accelerometer*, Michael Hutchinson .
- 170 [Galbraith and Hayward] ‘Development of a PVDF membrane hydrophone for use in air-coupled ultrasonic  
171 transducer calibration’. W Galbraith , G Hayward . *IEEE Transactions on Ultrasonics, Ferroelectrics, and*  
172 *Frequency Control* 45 (6) p. .
- 173 [Gonnet et al.] ‘Dielectric studies of PVDF crystallization. Application to in-situ monitoring in injection molding’.  
174 J M Gonnet , J Guillet , G Boiteux , R Fulchiron , G Seytre . *IEEE Transactions on Dielectrics and Electrical*  
175 *Insulation* 8 (6) p. .
- 176 [Rajala and Lekkala ()] ‘Film-Type Sensor Materials PVDF and EMFI in Measurement of Cardiorespiratory  
177 Systems -A Review’. S Rajala , J Lekkala . *IEEE Sensors Journal* 1996. 12. Penn State University
- 178 [Measurement Specialties, Inc. Piezo Film Sensors Technical Manual ()] *Measurement Specialties, Inc. Piezo*  
179 *Film Sensors Technical Manual*, 1998. Valley Forge, PA.
- 180 [Bauer] ‘PVDF shock sensors: applications to polar materials and high explosives’. F Bauer . *IEEE Transactions*  
181 *on Ultrasonics, Ferroelectrics and Frequency Control* 47 (6) p. .
- 182 [Bauer (2000)] ‘PVDF Shock Sensors: applications to polar materials and high explosives’. F Bauer . *IEEE*  
183 *Transactions on Ultrasonics, Ferroelectrics, and Frequency Control* November 2000.
- 184 [Barsky et al.] ‘Robot gripper control system using PVDF piezoelectric sensors’. M F Barsky , D K Lindner , R  
185 O Claus . *IEEE Transactions on Ultrasonics, Ferroelectrics, and Frequency Control* 36 (1) p. .
- 186 [The Electrical Engineering Handbook 14. Sedra and Smith ()] *The Electrical Engineering Handbook 14. Sedra*  
187 *and Smith*, 1989. 1993. 2015. New York; Ann Arbor, MI: CRC Press.
- 188 [Selfridge and Lewin] ‘Wideband spherically focused PVDF acoustic sources for calibration of ultrasound  
189 hydrophone probes’. A Selfridge , P A Lewin . *IEEE Transactions on Ultrasonics, Ferroelectrics and Frequency*  
190 *Control* 47 (6) p. .